SAND2016-1725C

Large-eddy simulation of soot development in a piloted jet flame with radiation

R. Knaus* and J. C. Hewson

1. Abstract

The generation of soot during a fire can strongly effect the overall behavior, largely through the enhanced radiative heat loss associated with the soot temperature field interactions. A large-eddy simulation of a nonpremixed ethylene-air piloted jet simulation (the Shaddix burner, Re=20,000) is performed using a two-equation soot model based on a nonadiabatic flamelet library and a coupled radiation model (discrete ordinates). Predictions of soot volume fraction are discussed, as well as the sensitivity of the soot volume fraction to the parameters of the two-equation soot model. The results are also compared with an eddy-dissipation concept based soot model and experimental data.

2. Introduction

In hydrocarbon flames where the residence time is significant, as occurs in fires and large-scale combustors, a significant fraction of the fuel carbon can be converted to soot. Most soot is oxidized in engineered combustors, but any soot emitted from the flame is a significant pollutant [1]. Soot in and around flames also plays an important role in radiative heat transfer. The overlap of the soot with high temperature flame zones is an important source of radiant flux and soot advected to cooler flame regions is an important absorber of this radiant flux. This radiant flux redistributes energy in fires, but the flux that reaches solid or liquid fuels is of even greater importance because this thermal energy acts to vaporize or pyrolyze these fuels.

Soot is known to evolve slowly relative to most of the main combustion chemistry [2] so that quasi-steady assumptions, as typical in flamelet model, for example, are not generally accurate for predicting soot volume fractions However, those components of the soot source terms that depend on the main flame chemistry have been expressed using flamelet libraries with some success [3, 4]. This led to a series of two-equation soot models being developed on a semi-empirical basis [5, 6, 7]. Most of the previous predictions have used Reynolds-averaged Navier-Stokes (RANS) approaches that involve a convolution of the source term over the variance of the mixture composition [3, 4, 8]. More recently, large-eddy simulations (LES) have been employed to model soot evolution [9, 10].

In the present work, we focus on investigating the co-evolution of the soot and the enthalpy field using both RANS and LES with a flamelet library to model the main flame chemistry including soot and enthalpy (radiation) source terms. RANS-based flamelet approaches are designed to integrate over unresolved fluctuations using presumed forms of the probability density function (pdf) such

*Corresponding author: rcknaus@sandia.gov

that only an average state is evolved. In LES a fraction of the fluctuations are resolved, and the objective here is to understand the role of fluctuations on the overall evolution. Because many interactions are nonlinear, it can be expected that resolving a fraction of the fluctuations can lead to a potentially richer range of behavior.

3. Soot-radiation modeling

Predictions of a turbulent ethylene jet flame are conducted using an unstructured control-volume finite-element code [11, 12], a component of Sandia National Laboratories Sierra thermal-fluids code suite. In addition to the filtered Navier-Stokes equations, filtered equations for the mixture fraction, the enthalpy and additional soot variables are evolved with a standard Smagorinski model for subgrid processes. RANS simulations are also conducted where a standard k-ϵ-$\widetilde{Z"^2}$ model is used to describe the fluctuations.

Required fluid properties (e.g.density and temperature) are obtained as a function of the mixture fraction and the enthalpy as well as approximations for the scalar dissipation rate and mixture fraction variance obtained using standard processes for the Smagorinski closure. These properties are obtained using flamelet calculations over a range of scalar dissipation rates and heat losses; adiabatic quasi-steady flamelets provide initial conditions to the transient evolution of flamelets with heat losses that are significant enough to transiently extinguish the flamelets in a manner that is set to represent radiative extinction. These unsteady flames have an enthalpy deficit, the difference between the stoichiometric enthalpy adiabatic and non-adiabatic values, that forms one of the dimensions of the flamelet table library. The authors use a modified version of the FlameMaster code [13] to generate the steady and unsteady flamelets. In addition to basic fluid properties, the quasi-steady main-flame contributions to source terms for soot and radiation are also computed using these flamelet models. With an estimate for the mixture fraction variance, a presumed form (clipped Gaussian) of the subgrid mixture fraction pdf is used to convolve flamelet quantities over the expected distribution of states. This is particularly important for RANS simulations as will be discussed below, but the variance of other variables beyond the mixture fraction is neglected. The method for obtaining these quantities is further described in the next section.

We use a two-equation soot model, transporting both the number density of soot as well as its mass concentration, to describe the development of soot in the LES.

$$\frac{\partial \bar{\rho}\tilde{N}}{\partial t} + \nabla \cdot (\bar{\rho}\mathbf{u}\tilde{N}) = \nabla \cdot \left(\frac{\mu}{\mathrm{Sc}_{\mathrm{turb.}}} \nabla N \right) + (\mathrm{Nucl.}) + (\mathrm{Coag.})\tilde{N}^{11/6}\tilde{M}^{1/6} \tag{1}$$

$$\frac{\partial \bar{\rho}\tilde{M}}{\partial t} + \nabla \cdot (\bar{\rho}\mathbf{u}\tilde{M}) = \nabla \cdot \left(\frac{\mu}{\mathrm{Sc}_{\mathrm{turb.}}} \nabla \tilde{M} \right) + W_p(\mathrm{Nucl.}) + ((\mathrm{Surf.}) - (\mathrm{Oxid.}))\tilde{N}^{1/3}\tilde{M}^{2/3} \tag{2}$$

$$\tag{3}$$

The source terms—(Nucl.), (Coag.), (Surf.), and (Oxid.)—refer to the nucleation, coagulation, surface growth and oxidation processes respectively and are modeled according to the parameters given by Aksit and Moss [7]. The original OH oxidation term was augmented with the O_2 oxidation from Leung et al. [5]. For the LES, values of the soot source terms are read from the tabulated results of an ensemble of flamelet calculations, after convolution with a presumed PDF, clipped-Gaussian model for subgrid mixing.

The flow and soot evolution is coupled to participating-media radiation so that the enthalpy can evolve in a realistic manner. The absorptivity of soot (from Hubbard and Tien [14]) is added to the

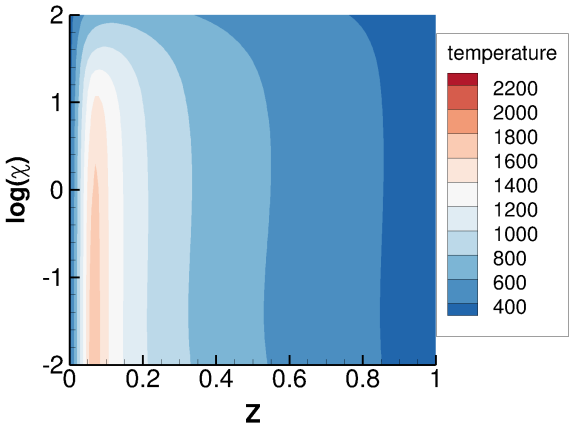

Figure 1: A 2D-slice from the 4-dimensional table, at zero scalar variance showing temperature in units Kelvin. The table data contains sharp regions where a high amount of resolution is required and relatively smooth regions where less resolution is required.

absorptivity of the gas (based on fits to Radcal results) and a discrete-ordinates solve using a 12^{th} order level-weighted, even moment quadrature was performed every 25 time-steps. The resulting enthalpy defect (the radiative loss in the enthalpy equation) is one of the independent variables for tabulated flamelet libraries, coupling the radiative loss to the thermochemical state of the gas in the large-eddy and RANS simulation.

4. Flamelet table coarsening

The flamelet table described above is a four-dimensional table (mixture fraction, mixture fraction variance, scalar dissipation, and enthalpy defect). This level of detail was employed to model the interaction of mixing, soot evolution and enthalpy evolution through radiative transport. An example of a two-dimensional slice of this four dimensional table is given in Figure 1. With higher dimensional tables, the overall size with even moderate resolution can be very large and take up a substantial amount of memory (gigabytes). While some intuition exists as to the resolution requirements of the higher-dimensional tables—e.g.more resolution in the mixture fraction dimension, where there is often a sharp dependence for computing soot source terms, than the scalar dissipation direction where the data is more smooth, see Figure 1—it is difficult to estimate the resolution requirements for each table variable in each direction.

Moreover, the resolution of the raw table data, the incoming flamelet predictions, is driven by resolution requirements for solving a system of PDEs including all source terms for all species. Only a subset of these quantities and source terms are required as dependent table variables, so the initial flamelet resolution is not necessarily pertinent for interpolating the solution during a large-eddy simulation. Assuming an abundance of data, we can coarsen sections of the table for each dependent variable (e.g.temperature) to a specifiable error norm relatively to the assumed fine initial table data. We use four-dimensional tensor-product cubic splines to interpolate the data and use an error indicator proportional to the error estimate for the splines. A fraction of the mesh points where the solution is best fit by cubic splines are removed, the spline coefficients recomputed, and the maximum error introduced by the coarsening is determined. If the error is

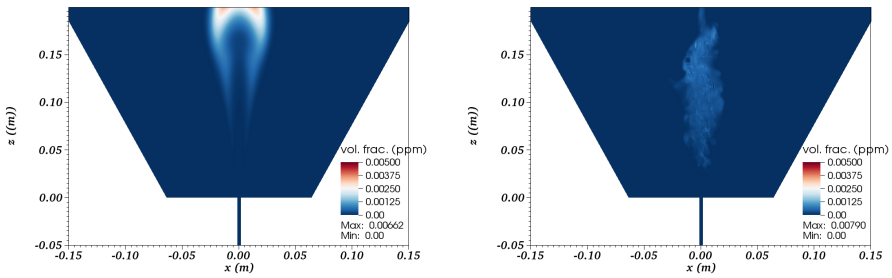

(a) RANS (b) LES

Figure 2: Soot volume fraction from the RANS and LES calculations. LES and RANS results are in progress and only the near field is shown.

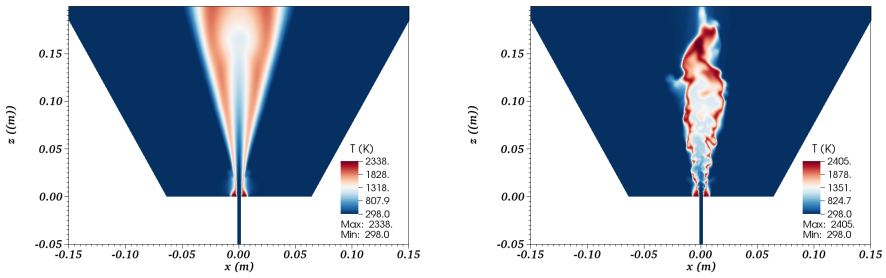

(a) RANS (b) LES

Figure 3: Temperature from the RANS and LES calculations. LES and RANS results are in progress and only the near field is shown.

below the specified tolerance, then the coarsening trial is accepted and we iteratively try to delete more mesh points, reducing the number of trial deletions until the maximum tolerance is reached. This process results in a significant reduction in the overall table size (a factor of 6 from a 3 gigabyte table to a 500 megabyte table) if allowing for up to a 0.5% error and a factor of twenty for a 1.5% error. Interesting questions regarding the necessary resolution and smoothness of the interpolation for thermochemical state data remain open. High degrees of accuracy are likely warranted for quantities like the density that are well understood and integral to the flow evolution. Some terms like the soot source terms have larger uncertainties. We note that it is important to differentiate between numerical and physics-based model form errors; it is preferable to minimize the relative numerical errors, but these are minimized in the context of the overall sum of the errors and reducing them to a small fraction of the physics-based modeling errors is appropriate for balancing computational effort.

5. Problem description

We carry out simulations in a piloted turbulent ethylene jet flame configuration with a bulk Reynolds number of 20,000, referred to here as the Shaddix burner. This burner is of similar design

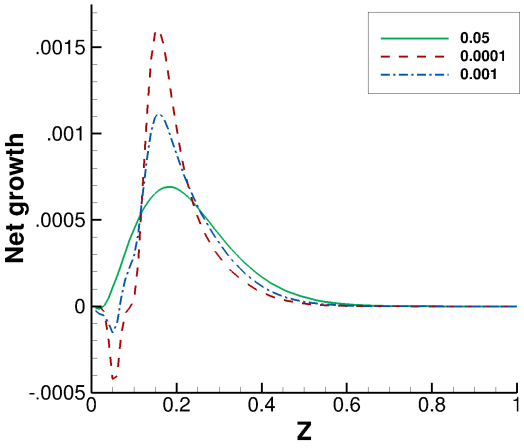

Figure 4: Net growth (surface growth - oxidation) at three different levels of scaled scalar variance from a flamelet simulation

to those used for other piloted jet flame measurements at Sandia National Laboratories, but the original design is from the University of Sydney. The Shaddix burner is a piloted ethylene jet with a diameter of $d_j = 3.2$ mm. The bulk velocity of the main jet is 54.7 m/s, the pilot has a bulk velocity of 5.8 m/s, and coflow speed of 0.9 m/s. For details on the geometry of the burner the reader is referred to [15]. The domain was meshed over a length of $400d_j$, with a conical outer jet extent initially at $20d_j$ and ultimately at approximately $200d_j$. The mesh resolution in the core of the jet was approximately $h = 0.05d_j$ with the mesh stretched in the radial and axial directions further into the domain, making for approximately 2 million total nodes. As described in the Soot-radiation modeling section, the simulations are carried out using a component of Sandia's Sierra thermal-fluid code suite; this component is referred to as Fuego and it provides control-volume finite-element discretization over an unstructured mesh. A backward-Euler time integration scheme was combined with a second-order control volume finite element discretization to integrate the mass, momentum, enthalpy, mixture fraction, and soot equations. To allow for the development of turbulence in the inflowing jet, the jet pipe was also modeled for 30 d_j upstream of the exit. Azimuthal disturbances were injected at the base of the pipe in order to transition the jet to a turbulent state.

6. Results

The simulations are still in progress and we intend to extend toward uniformly refining the simulations while evaluating the effect of resolution of the predictions of soot using the two-equation soot model. In addition to the LES, we have conducted RANS simulations of the same flame.

As the large-eddy simulation is still developing, we compare data from the near field of the turbulent jet, where the flow time scale is much shorter. In this region of the flow, the scaled scalar variance, $\widetilde{Z"^2}/\tilde{Z}(1-\tilde{Z})$, for the RANS simulation is relatively high (about 0.05 about the stoichiometric surface; c.f. Figure 4). The LES resolves much of the mixture fraction fluctuations so that the filtered mixture fraction variance is more than an order of magnitude smaller than

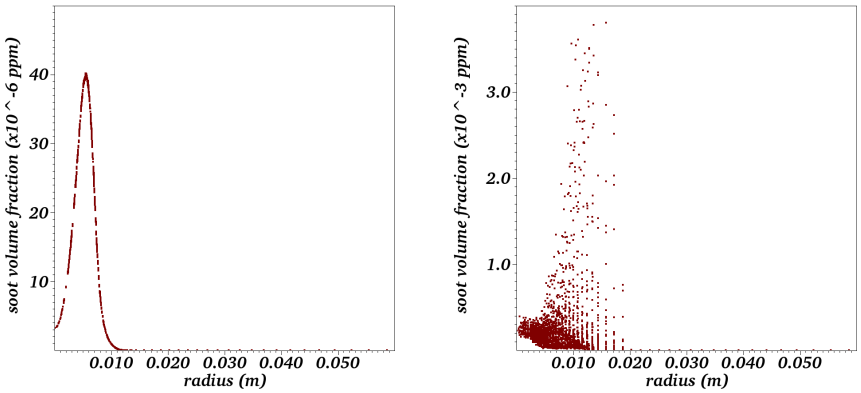

(a) RANS

(b) LES

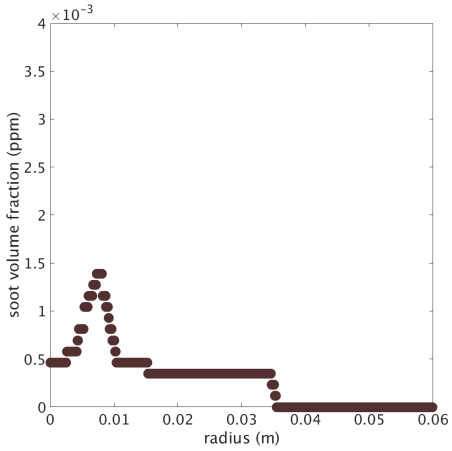

(c) Measurements from Ref. [16]

Figure 5: Soot volume fraction from the RANS and LES calculations, from a plane near the beginning of the jet (0.075m). Note that different scales are used between the RANS and LES data.

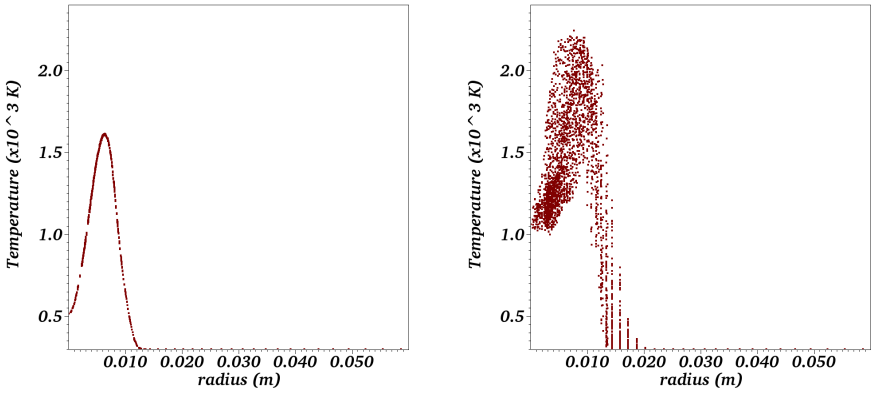

(a) RANS (b) LES

Figure 6: Temperature from the RANS and LES calculations, from a plane near the beginning of the jet (0.075m)

the RANS. In this near-source region, the mixing in the RANS calculation averages over both the oxidation and growth terms in the soot mass concentration evolution, resulting in the lack of a distinct oxidation regime in mixture fraction space as shown in Figure 4. The LES calculation, however, can capture some of the mixing in the turbulent flow, leading to distinct oxidation and surface growth regimes in mixture fraction space in the early development region of the jet.

This effect can lead to large excursions from the mean soot volume fraction in the LES relative to the RANS, as seen in Figure 5 and 2. The large excursions can then couple with the radiation solve and can potentially add additional variability in temperature field (Figures 6 and 3). In turn, the temperature couples with the soot predictions further downstream, with a relatively small upstream error in the temperature resulting in a much larger error in soot predictions [17].

7. Conclusions

Large-eddy simulations are in progress to address the sensitivity of soot predictions to resolution in large-eddy simulation as well as to the soot rates. An automatic table coarsening algorithm has been developed in order to reduce the memory consumption of the higher-dimensional table data required to parameterize the flame microstructure in a multiphysics environment. Preliminary results show substantial intermittency in the soot predictions for the large-eddy simulation even at a relatively coarse resolution and further work will be performed as the LES simulations reach a statistically-stationary state.

Acknowledgments

This material is based in part upon work supported in part by the National Science Foundation under Grant No. CBET-1403403 and supported by the Department of Energy National Nuclear Security Agency's Advanced Simulation and Computing Physics and Engineering Models Program at Sandia National Laboratories. Sandia National Laboratories is a multi-program laboratory managed and operated by Sandia Corporation, a wholly owned subsidiary of Lockheed Martin

Corporation, for the U.S. Department of Energy's National Nuclear Security Administration under contract DE-AC04-94AL85000.

[1] U. E. P. Agency, Air quality criteria for particulate matter, 204.

[2] J. H. Kent, D. Honnery, Soot and mixture fraction in turbulent diffusion flames, Combust. Sci. Tech. 54 (1987) 383–397.

[3] J. J. Young, J. B. Moss, Modelling sooting turbulent jet flames using an extended flamlet technique, Combust. Sci. Tech. 105 (1995) 33–53.

[4] S. J. Brookes, J. B. Moss, Predictions of soot and thermal radiation properties in confined turbulent jet diffusion flames, Combust. Flame 116 (1999) 486–503.

[5] K. M. Leung, R. P. Lindstedt, W. Jones, A simplified reaction mechanism for soot formation in nonpremixed flames, Combustion and flame 87 (1991) 289–305.

[6] P. R. Lindstedt, Simplified soot nucleation and surface growth for nonpremixed flames, in: H. Bockhorn (Ed.), Soot Formation in Combustion, volume 59 of *Chemical Physics*, Springer-Verlag, 1994, pp. 417–439.

[7] I. Aksit, J. Moss, A hybrid scalar model for sooting turbulent flames, Combustion and flame 145 (2006) 231–244.

[8] H. Pitsch, E. Riesmeier, N. Peters, Unsteady flamelet modeling of soot formation in turbulent diffusion flames, Combust. Sci. Tech. 158 (2000) 389–406.

[9] M. E. Mueller, H. Pitsch, Large eddy simulation of soot evolution in an aircraft combustor, Physics of Fluids (1994-present) 25 (2013) 110812.

[10] Y. Xuan, G. Blanquart, Effects of aromatic chemistry-turbulence interactions on soot formation in a turbulent non-premixed flame, Proceedings of the Combustion Institute 35 (2015) 1911–1919.

[11] S. R. Tieszen, S. Domino, A. R. Black, Validation and uncertainty quantification of Fuego simulations of calorimeter heating in a wind-driven hydrocarbon pool fire, Technical Report SAND2009-7605, Sandia National Laboratories, Albuquerque, NM, 2009.

[12] A. Hanlin, S. Domino, V. Figueroa, V. Romero, Validation and uncertainty quantification of Fuego simulations of calorimeter heating in a wind-driven hydrocarbon pool fire, Technical Report SAND2009-7605, Sandia National Laboratories, Albuquerque, NM, 2009.

[13] H. Pitsch, Flamemaster: A c++ computer program for 0d combustion and 1d laminar flame calculations, Cited in (1998) 81.

[14] G. Hubbard, C. Tien, Infrared mean absorption coefficients of luminous flames and smoke, Journal of Heat Transfer 100 (1978) 235–239.

[15] C. R. Shaddix, J. Zhang, Joint temperature-volume fraction statistics of soot in turbulent non-premixed jet flames., in: Proceedings of the 8th US Combustion Meeting, 2013.

[16] C. R. Shaddix, T. C. Williams, J. Zhang, Quantitative soot concentration measurements in turbulent non-premixed jet flames of ethylene and a jet fuel surrogate, Proc. Combust. Instit. (submitted 2015).

[17] M. E. Mueller, V. Raman, Effects of turbulent combustion modeling errors on soot evolution in a turbulent nonpremixed jet flame, Combustion and Flame 161 (2014) 1842–1848.